

AD-A078 442

ANALYTICAL MECHANICS ASSOCIATES INC JERICO NY
PREFERENCE-ORDERED DISCRETE-GAMING ANALYSIS OF AIR-TO-AIR COMBA--ETC(U)
JUN 79 H J KELLEY , L LEFTON

F/G 12/1

F33615-77-C-3144

UNCLASSIFIED

AFFDL-TR-79-3057

NL

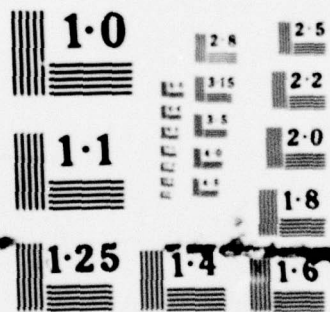
1 OF 1
AD-
A 078442



END
DATE
FILMED

1 - 80

DOC



NATIONAL BUREAU OF STANDARDS
MICROCOPY RESOLUTION TEST CHART

② LEVEL II

AFFDL-TR-79-3057 ✓

ADA 078442

PREFERENCE-ORDERED DISCRETE-GAMING ANALYSIS OF AIR-TO-AIR COMBAT

Henry J. Kelley
Leon Lefton

Analytical Mechanics Associates, Inc. ✓
Jericho, New York 11753

JUNE 1979

DDC
RECEIVED
DEC 17 1979
B

Final Report

September 1977 - May 1979

DDC FILE COPY

Approved for public release; distribution unlimited.

AIR FORCE FLIGHT DYNAMICS LABORATORY
AIR FORCE WRIGHT AERONAUTICAL LABORATORIES
AIR FORCE SYSTEMS COMMAND
WRIGHT-PATTERSON AIR FORCE BASE, OHIO 45433

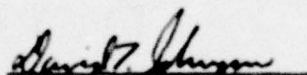
79 13 11 089


NOTICE

When Government drawings, specifications, or other data are used for any purpose other than in connection with a definitely related Government procurement operation, the United States Government thereby incurs no responsibility nor any obligation whatsoever; and the fact that the Government may have formulated, furnished, or in any way supplied the said drawings, specifications, or other data, is not to be regarded by implication or otherwise as in any manner licensing the holder or any other person or corporation, or conveying any rights or permission to manufacture, use, or sell any patented invention that may in any way be related thereto.


This report has been reviewed by the Information Office (OI) and is releasable to the National Technical Information Service (NTIS). At NTIS, it will be available to the general public, including foreign nations.

This technical report has been reviewed and is approved for publication.


David T. Johnson
Project Engineer


Melvin L. Buck
Chief, High Speed Aero. Perf. Br.

FOR THE COMMANDER


Peter J. Butkewicz
Colonel, USAF
Chief, Aeromechanics Division

If your address has changed, if you wish to be removed from our mailing list, or if the addressee is no longer employed by your organization, please notify AFFDL/FXG, W-PAFB, OH 45433 to help us maintain a current mailing list.

Copies of this report should not be returned unless return is required by security considerations, contractual obligations, or notice on a specific document.

REFERENCES (cont'd)

7. Newberry, C. H. ; Discussions at USAF Weapons Laboratory, Kirtland AFB, New Mexico, mid-1976.
8. Kopp, R. E. ; "The Numerical Solution of Discrete Dynamic Combat Type Games," in Techniques of Optimization, A.V. Balakrishnan, ed. , Academic Press, New York, 1972.
9. Isaacs, R. ; Differential Games, Wiley, New York, 1955.
10. Isaacs, R. ; "The Past and Some Bits of the Future," in The Theory and Application of Differential Games, J.D. Grote, ed. , Reidel, Dordrecht, 1975.
11. Friedman, A. ; Differential Games, Wiley-Interscience, New York, 1971.
12. Private communication with Gary Hill (NASA-Ames engineer and A-7 pilot), April 1976.
13. Kelley, H. J. and Lefton, L. ; "Estimation of Weapon-Radius Versus Maneuverability Tradeoff for Air-to-Air Combat," ALAA Journal, Vol. 15, No. 2, February 1977.
14. Mummolo, F. and Lefton, L. ; "Cubic Splines and Cubic-Spline Lattices for Digital Computation," Analytical Mechanics Associates, Inc. , Report Number 72-28, July 1972, revised December 1974.

UNCLASSIFIED

SECURITY CLASSIFICATION OF THIS PAGE (When Data Entered)

19 REPORT DOCUMENTATION PAGE		READ INSTRUCTIONS BEFORE COMPLETING FORM
1. REPORT NUMBER 18 AFFDL-TR-79-3057	2. GOVT ACCESSION NO.	3. RECIPIENT'S CATALOG NUMBER
4. TITLE (and Subtitle) 6 PREFERENCE-ORDERED DISCRETE-GAMING ANALYSIS OF AIR-TO-AIR COMBAT	5. TYPE OF REPORT & PERIOD COVERED 9 Final Rept. 24 Sep 77 - May 79	6. PERFORMING ORGANIZATION REPORT NUMBER
7. AUTHOR(s) 10 Henry J. Kelley Leon Lefton	8. CONTRACT OR GRANT NUMBER(s) 15 F 33615-77-C-3144	
9. PERFORMING ORGANIZATION NAME AND ADDRESS Analytical Mechanics Associates, Inc. 50 Jericho Turnpike, Jericho, N. Y. 11753	10. PROGRAM ELEMENT, PROJECT, TASK AREA & WORK UNIT NUMBERS 16 2404-07-11	17 07
11. CONTROLLING OFFICE NAME AND ADDRESS Air Force Flight Dynamics Laboratory (FXG) Wright-Patterson AF Base, Ohio 45433	12. REPORT DATE 11 Jun 79	13. NUMBER OF PAGES 67
14. MONITORING AGENCY NAME & ADDRESS (if different from Controlling Office) 12 67 PE 6221 F 405 562	15. SECURITY CLASS. (of this report) Unclassified	15a. DECLASSIFICATION/DOWNGRADING SCHEDULE
16. DISTRIBUTION STATEMENT (of this Report) Approved for public release; distribution unlimited.		
17. DISTRIBUTION STATEMENT (of the abstract entered in Block 20, if different from Report)		
18. SUPPLEMENTARY NOTES		
19. KEY WORDS (Continue on reverse side if necessary and identify by block number) air-to-air-combat analysis, differential games, pursuit/evasion, threat-reciprocity, reprisal strategy.		
20. ABSTRACT (Continue on reverse side if necessary and identify by block number) A preference-ordered discrete-gaming air-to-air-combat model is described. Approximately optimal switchings between several closed-loop control policies is provided by an active-cell structure in the state space, which is divided into regions of draw outcome and various types of capture. Cell buildup technique is discussed and the results of computations for families of duels presented. A threat-reciprocity scheme for characterizing draw outcomes and tactics is discussed. A reprisal-strategy scheme for exploiting opponent's errors by extrapolation is described.		

DD FORM 1 JAN 73 1473 EDITION OF 1 NOV 65 IS OBSOLETE

UNCLASSIFIED

SECURITY CLASSIFICATION OF THIS PAGE (When Data Entered)

405 562

FOREWORD

The research presently reported was supported by USAF Flight Dynamics Laboratory, Wright-Patterson AFB, Ohio under Contract F33615-77-C-3144 over the period 20 September 1977 to 20 May 1979. The technical monitors were Dr. L. Earl Miller and Mr. David Johnson of AFFDL/FXG. The research is a continuation of that reported in Ref. 1, initiated in an effort for USAF Weapons Laboratory, Kirtland AFB, New Mexico (AFWL/PGA).

ACCESSION by	
NTIS	White Section <input checked="" type="checkbox"/>
DDC	Buff Section <input type="checkbox"/>
UNANNOUNCED	<input type="checkbox"/>
JUSTIFICATION	
BY	
DISTRIBUTION/AVAILABILITY CODES	
Dist. Avail. and/or SPECIAL	
A	

TABLE OF CONTENTS

SECTION		PAGE
I	INTRODUCTION	1
II	VEHICLE MODELING	2
III	CAPTURE CRITERIA	4
IV	PREFERENCE ORDERING	5
V	DRAW-SPACE INDICES	6
VI	DISENGAGEMENT	9
VII	CELL BUILDUP TECHNIQUE	10
VIII	CELL INTERPOLATION LOGIC	14
IX	DESCRIPTION OF EXAMPLES	17
X	SCORING	18
XI	GAME-SCORING ILLUSTRATIONS	20
XII	RESULTS FOR A FIRST EXAMPLE	24
XIII	REPRISAL GUIDANCE	29
XIV	ILLUSTRATIVE NUMERICAL RESULTS FOR REPRISAL GUIDANCE	31
XV	ALTITUDE CHOICE AND "MAKING USE OF THE VERTICAL"	33
XVI	POINT-MASS SIMULATION	37
	1 Equations of Motion	37
	2 Data Representation	38
	3 Bank-Angle Logic	39
XVII	CELL BUILDUP AND EVALUATION PROGRAM	42
XVIII	INPUT	44
XIX	CONCLUDING REMARKS	48
	REFERENCES	56

LIST OF ILLUSTRATIONS

FIGURE		PAGE
1	Generalized Miss	50
2	Capture and Draw Regions in \bar{Q}_1, \bar{Q}_2 Space	51
3	Maneuver Sketches for Matrix Elements of Gaming Example - #1 Heading 2.4 rad. , #2 Heading -1.18 rad.	52
4	Maneuver Sketches for Matrix Elements of Gaming Example - #1 Heading 1.96 rad. , #2 Heading -.26 rad.	53
5	Trajectory Comparison	54
6	Breakaway Miss vs Altitude	55

LIST OF TABLES

TABLE		PAGE
1	EFFECT OF WIDE-ANGLE WEAPONRY	24
2	EFFECT OF MUTUAL-CAPTURE PERIOD	25
3	EFFECT OF TURN-AND-DASH-AWAY OPTION	26
4	EFFECT OF ACTIVE-CELL STRUCTURE	26
5	EFFECT OF INITIAL SEPARATION DISTANCE	27
6	EFFECT OF GUIDANCE OPTIONS	31

SYMBOLS

x_1, y_1	horizontal position components, Vehicle #1
x_2, y_2	horizontal position components, Vehicle #2
V_1, V_2	speeds of Vehicles #1 and #2
χ_1, χ_2	heading angles, Vehicles #1 and #2
ω_1, ω_2	turn rates, Vehicles #1 and #2
C	navigation ratio
r, θ	polar coordinates of Vehicle #1 relative to Vehicle #2, defined by eqs. (10) and (11)
σ	weapon angular trainability limit
Q_1, Q_2	extended-weapon-envelope functions for capture by player #1 and player #2. See Fig. 1
\bar{Q}_1, \bar{Q}_2	generalized miss quantities defined by eq. (13)
Q^*	generalized-miss difference $\bar{Q}_1 - \bar{Q}_2$
ζ	interpolation scalar
z_i	normalized state increments employed for interpolation in cell structure
p_i	switch-surface indices
\bar{R}	game-of-two-cars miss estimate defined by eq. (14)
h	altitude
V	velocity
E	specific energy $h + \frac{V^2}{2g}$
γ	path angle to horizontal
μ	bank angle

η	throttle setting
L	lift
D	drag
α	angle of attack
$\hat{C}_L(M)$	aerodynamic limit on lift coefficient, Mach-number dependent
C_{L_M}	lift-coefficient limit, the lesser of aerodynamic and structural limits

SUMMARY

Results are presented for the development of a preference-ordered discrete-gaming air-to-air-combat model. A parameterized model was employed featuring gaming choice between several closed-loop control policies, approximately optimal switchings between policies being provided by an active-cell structure in the state space, which is divided into regions of two types of draw and three types of capture. The technique for building up the aggregation of active cells received much attention. A cell structure was adopted in which cells in the state space are partitioned in terms of elapsed time from the initiation of an encounter, this being relevant to control-policy choice through the definition of a draw outcome in terms of elapsed time. The buildup technique evolved adds one cell at a time to the aggregation of active cells. It turns out that few additional capture cells are accumulated past 15 or 20 sec. elapsed time, and that the 30 sec. maximum time employed in most of the example computations may have been excessive. The preference-ordered gaming technique is described in Ref. 1, generated in part during an antecedent effort for NASA-Ames and AFWL. Much of the material of Ref. 1 has been included in the present report in the interest of a reasonably self-contained presentation.

The body of this report contains sections dealing with cell buildup technique, examples of preference-ordered scoring of the game matrix, graduation of draw outcomes via a threat-reciprocity concept, a reprisal-strategy scheme which exploits opponent's errors by extrapolation, choice of altitude for 3-D modeling and a description of point-mass simulation model making use of data from gaming models for control logic.

SECTION I

INTRODUCTION

A capability has evolved for the solution of pursuit/evasion differential games with vehicle models sufficiently realistic to be of some practical interest. However, the literature focuses almost entirely on the case of an evader undefended save for evasive maneuvering, and has only limited applicability to air combat between aircraft of roughly equal capability. One approach to this situation which has received some attention is the calculation of outcomes with pursuit and evasion rôles assigned and again with them interchanged, then the use of these to define surfaces separating win, lose, and draw regions (Refs. 2,3). This approach leads to ambiguous results with large-envelope weaponry, which produces a large mutual-capture region when the assumption of pursuit irrespective of the consequences is maintained. A technical approach to preliminary maneuvering in the face of possible draw and/or mutual capture has been examined conceptually in Ref. 4 and is developed in a preliminary way in the presently reported effort.

Present focus is on analyzing the first few seconds of a one-on-one air engagement using rather crude physical modeling and control logic, but emphasizing rational choice between strategies, according to player preference among outcomes: win, loss, mutual capture, purposeful disengagement, draw. The preference-ordering formulation is due to M. Falco (Ref. 5). The approach presently explored cannot be expected to be very satisfactory for protracted air duels, e.g., "dogfighting" with gun armament; it is a creature of large-envelope weaponry.

SECTION II

VEHICLE MODELING

Planar motion of two constant-speed vehicles is described by the equations:

$$\dot{x}_1 = V_1 \sin \chi_1 \quad (1)$$

$$\dot{y}_1 = V_1 \cos \chi_1 \quad (2)$$

$$\dot{x}_2 = V_2 \sin \chi_2 \quad (3)$$

$$\dot{y}_2 = V_2 \cos \chi_2 \quad (4)$$

$$\dot{\chi}_1 = \omega_1 \quad (5)$$

$$\dot{\chi}_2 = \omega_2 \quad (6)$$

Steering by proportional navigation with bounded turn-rate provides aggressor options:

$$\begin{aligned} \omega_1 &= -\bar{\omega}_1 & \text{if } \omega_1^* \leq -\bar{\omega}_1 \\ &= \omega_1^* & \text{if } -\bar{\omega}_1 \leq \omega_1^* \leq \bar{\omega}_1 \\ &= \bar{\omega}_1 & \text{if } \bar{\omega}_1 \leq \omega_1^* \end{aligned} \quad (7)$$

$$\omega_1^* = C \dot{\theta}$$

and $C > 0$ is the so-called navigation ratio.

A defensive option is provided by turn-and-dash-away guidance, which effects a turn away from the sightline direction, bringing the vehicle's velocity vector anti-parallel to the sightline. In this case, ω_1^* , appearing in (7), is given by

$$\omega_1^* = -C \bar{\omega}_1 \left[\frac{(x_2 - x_1)}{r} \cos \chi_1 - \frac{(y_2 - y_1)}{r} \sin \chi_1 \right] \quad (8)$$

$$\text{if} \left[\frac{(x_2 - x_1)}{r} \sin \chi_1 + \frac{(y_2 - y_1)}{r} \cos \chi_1 \right] \leq 0$$

$$\omega_1^* = -C \bar{\omega}_1 \text{signum} \left[\frac{(x_2 - x_1)}{r} \cos \chi_1 - \frac{(y_2 - y_1)}{r} \sin \chi_1 \right] \quad (9)$$

$$\text{if} \left[\frac{(x_2 - x_1)}{r} \sin \chi_1 + \frac{(y_2 - y_1)}{r} \cos \chi_1 \right] > 0$$

Similar offensive and defensive options provided the second aircraft define ω_2 .

Relative polar coordinates r, θ are useful, and are given by:

$$r = \sqrt{(x_1 - x_2)^2 + (y_1 - y_2)^2} \quad (10)$$

$$\theta = \arctan \frac{x_1 - x_2}{y_1 - y_2} \quad (11)$$

SECTION III

CAPTURE CRITERIA

Weapon envelopes idealized in terms of a radius limit \bar{r} and an angular trainability limit σ are assumed in the illustrative examples to be presented, although the computational approach also lends itself to more realistic envelopes. Thus, Vehicle #1 captures Vehicle #2 when $r \leq \bar{r}$, and

$$-(\sin \theta \sin \chi_1 + \cos \theta \cos \chi_1) \geq \cos \sigma_1 \quad (12)$$

The description of Vehicle #2's weapon envelope employs a similar form; however, the example computations will employ a composite of circular segments for two weapons of differing lethal radii and angular limits for Vehicle #2.

SECTION IV

PREFERENCE ORDERING

If both aircraft are manned and only one (Vehicle #1) has the possibility of disengagement upward by virtue of higher ceiling, reasonable preference orders are 1,4,5,3,2 for Vehicle #1, and 2,5,4,3,1 for Vehicle #2, where the scoring is

- 1 : 1 captures
- 2 : 2 captures
- 3 : mutual capture
- 4 : 1 disengages
- 5 : draw

In the interest of more nearly unique determination of optimal control parameters, it is advantageous to adopt graduated preferences within each category, thus: minimax time in 1, maximin time in 2, maximum time in 3, minimax time in 4, minimax energy difference (in rough estimate) in 5.

SECTION V

DRAW-SPACE INDICES

Control logic for maneuvering in the draw region has received insufficient attention in the 2-D modeling of Ref. 1 and, for that matter, in air-combat modeling in general. The threat-reciprocity concept of Ref. 4 is of interest in this connection, and is developed further in the following. An appropriate measure of generalized miss is the extended-weapon-envelope idea of Roberts and Montgomery (Ref. 6) illustrated in Fig. 1. This offers miss measures suitable for use with the discrete-gaming model, the minima versus time of the generalized misses of the two combatants furnishing data for a scoring index in the draw region.

The functions Q_1 and Q_2 of the joint state describe extended weapon envelopes for the two players. $Q_1 \leq 0$ corresponds to the capture envelope of player #1 (Fig. 1); the function \bar{Q}_1 to

$$\bar{Q}_1 = \min_{0 \leq t \leq t_f} Q_1(t) \quad (13)$$

The generalized misses \bar{Q}_1 and \bar{Q}_2 are defined for any control histories, not necessarily optimal. In particular, they are defined for the trajectory pairs corresponding to each matrix element for which the outcome is a draw.

The following examination of control rationale, in the context of the preference ordering which is appropriate to combat between manned vehicles, is due to Eugene Cliff of Virginia Polytechnic Institute. The assumed preference ordering is 1,5,3,2 for player #1 and 2,5,3,1 for player #2. A 1 outcome denotes capture by player #1, a 2 by #2, 3 denotes mutual capture, and 5 a draw. The special type of draw designated 4 in Ref. 1 will figure in the first example to be presented, but not in the second.

If $\bar{Q}_2 \gg 0$, player #1 can be aggressive and minimize \bar{Q}_1 ; however, if $\bar{Q}_2 \cong 0$, then player #1 must evade and maximize \bar{Q}_2 . If $\bar{Q}_1 \gg 0$, then #2 can be aggressive and minimize \bar{Q}_2 ; however, if $\bar{Q}_1 \cong 0$, then player #2 must evade and maximize \bar{Q}_1 . Thus, there are four possible qualitative "states" and associated desires within the draw region.

A $\bar{Q}_1 \gg 0$ and $\bar{Q}_2 \gg 0$

#1 will min \bar{Q}_1

#2 will min \bar{Q}_2

B $\bar{Q}_1 \gg 0$ and $\bar{Q}_2 \cong 0$

#1 will max \bar{Q}_2

#2 will min \bar{Q}_2

C $\bar{Q}_1 \cong 0$ and $\bar{Q}_2 \gg 0$

#1 will min \bar{Q}_1

#2 will max \bar{Q}_1

D $\bar{Q}_1 \cong 0$ and $\bar{Q}_2 \cong 0$

#1 will max \bar{Q}_2

#2 will max \bar{Q}_1

This subdivision of the draw space is shown in Fig. 2, which also shows 1, 2, and 3 capture regions. In "states" B and C, zero-sum game theory "works" in that the players agree upon an objective, each in opposition to the other.

The threat-reciprocity concept blends the control policies in the draw space smoothly between the regions, in terms of the relative importance attached to \bar{Q}_1 and \bar{Q}_2 in each player's control choice. The implementation adopted in the presently reported first computational attempt, however, is much cruder than this. Essentially, it is the use of 0 and 1 weights in regions B, C, and D, as noted in the preceding listing, and the use of minimax $Q^* = \bar{Q}_1 - \bar{Q}_2$ in region A. The thresholds were set somewhat arbitrarily at $\bar{Q} = 1.2$.

SECTION VI

DISENGAGEMENT

The possibility of a deliberate disengagement, as distinct from an inconclusive draw, may be provided for under appropriate circumstances. One such, which is compatible with the present modeling, is the attainment of a large enough energy advantage, which, taken together with a substantial superiority in ceiling, permits escape upward. In the first example to be presented, Vehicle #1, which has less effective weaponry, has higher performance and the capability of disengaging upward by zooming, given sufficient specific energy, with the possibility of mounting a second attack subsequently.

Disengagement estimates are made very roughly, without actually integrating specific energy changes, by assuming that $|\omega| = \bar{\omega}$ along the entire trajectory. This is actually a fairly good assumption in the single-pass scenario of the present example. The choice of turn-rate bound involves possible sacrifice of energy rate for increasing turn rate, on account of maneuvering-drag build-up. Thus, a choice of the bounds $\bar{\omega}_1$ and $\bar{\omega}_2$ implies a time at which disengagement is possible, unless capture by Vehicle #2 has occurred earlier. Any less favorable outcome past this time is scored as a disengagement.

SECTION VII

CELL BUILDUP TECHNIQUE

A measure of optimization may be provided within the confines of the parameterization adopted, and other "coarseness-of-mesh" limitations, by use of Kopp's "backing-up" idea (Ref. 8). Switching between guidance modes and parameters is permitted both players at preset intervals. Optimal guidance choices are stored in cellular subdivisions of the joint state space (Ref. 5). Some optimal guidance choices are first determined for cells neighboring the target set by integration forward in time of short trajectory pairs, originating from their midpoints. These trajectories are terminated after three seconds. They are then scored as described in the preceding section. It can be argued that the preference-ordered matrix choice is optimal within the chosen parameterization, if the trajectories are sufficiently short and the cellular mesh is sufficiently fine. The optimal guidance choice is then stored for use subsequently during passage of trajectories through such a cell, now termed an "active" cell.

The data of the first three tables presented in the following section were obtained without the use of an active-cell structure — no guidance switchings. The results of Tables 4 and 5 were obtained with a cell structure comprised of 250 cells in the 3-space, each divided into ten subcells according to time remaining until attainment of the specified 30 sec. maximum time. A draw outcome from a matrix scored with short trajectories is used to activate only the short time-to-go subcells.

The simplified energy bookkeeping used for figuring disengagements is not compatible with the use of active-cell structure because the more intricate bookkeeping version, to which the combination leads, amounts to rough estimation of energy-modeled disengagements — five-state instead of three-state. Some experimentation of this kind has been done; however, disengagements were figured without guidance switchings in the results to be presented, i. e., the active-cell

guidance overridden. All disengagements are assumed to be initiated at time zero and are, in essence, decisions not to engage. This seems reasonable for scenarios in which both participants employ gaming logic, precluding blunders, although it would likely be unsatisfactory in other settings.

The variables of the joint state space are the separation distance, r , and the heading angles of the two vehicles measured from the line of sight. Each cell is divided into subcells according to time remaining until attainment of the specified maximum time; thus, in the first example, there are ten subcells. Development of cell buildup technique, since the work of Ref. 1 was carried out, has resulted in significant gains in computational efficiency and considerable simplification. The following description applies to the improved procedure, which employs a more rigid discretization than the former one: changes in guidance are implemented at three-second intervals and, similarly, captures are scored only at the mesh points. A major effect of the change is that trajectories generated in buildup calculations always find themselves in active subcells after the first three-second interval, and none need be discarded for passing through neutral subcells.

The cell buildup starts with three-second trajectories originating from the midpoints of target-set cells in order to determine which correspond to mutual captures. A dozen trajectories are generated from each, corresponding to various guidance combinations, as described in Ref. 1. The matrix scoring decides whether the subcell has a single-capture outcome or a mutual-capture outcome (determined by the occurrence of a second capture within three seconds). Target-set cells in a region of overlap of the two target sets can be scored without trajectory integrations, as the mutual-capture outcome is obvious at the outset. Such cells have the 3 outcome (mutual capture) in all ten subcells and no guidance choice stored, as the outcome is instantaneous and independent of guidance. For other target-set cells whose scoring results in a mutual-capture outcome within the three seconds, the subcells

are activated with 3 outcomes plus whatever guidance combination emerged from the matrix scoring. Next, a dozen three-second trajectories are run out of each cell, starting at time 27 sec., and scoring done via the matrix procedure. The trajectory emerging from the matrix scoring is termed a "lead trajectory". Trajectory integrations are continued until the maximum duration, 30 sec., if no capture has occurred by then, or until capture plus three seconds, in order to determine whether there is a mutual capture. Thus, some nominally three-second trajectories are actually six, etc. The continuing buildup employs progressively longer trajectories: six-second trajectories starting at 24 sec., etc. When a subcell is activated with a capture outcome, the same outcome and guidance are used to generate all of the longer-time-to-go subcells of the particular cell.

Active-cell data are ordinarily presented in three arrays of computer printout. The first two arrays relate cell number and cell content. The third array locates the cell in state space. The content of each subcell is represented by three digits, of which the first two are guidance (1 through 12) and the last is the outcome. The shortest-time-to-go subcell data appears on the left of the word in the second array, the longest on the right in the first array. Thus, the printout for cell #162

091 091 091 091 091

in the first array, and

015 015 015 091 091

in the second, indicates that, for the three shortest-time-to-go subcells, the outcome is 5 (a draw) and the guidance is 1, while for the seven longest-time-to-go subcells, the outcome is a 1-capture and the guidance 9.

The entry in the third array

1 0 9 0 5

indicates by its first digit, 1, that the separation between the two aircraft lies between 0 and .75 n.m.i. for the particular cell. The next two digits, 0 9, indicate that the function $\pi - \chi_1 + \theta$ of the first vehicle's heading relative to the sightline direction lies between 60° and 90° . The last two digits, 0 5, denote that $\chi_2 - \theta$ lies between 90° and 180° .

SECTION VIII

CELL INTERPOLATION LOGIC

The active-cell representation of guidance, described in the foregoing, forces guidance switchings to take place at cell interfaces, and produces a somewhat jagged approximation to a switching surface in the three-space. An improved representation using interpolation between cell midpoints is described in the following. The technique has not been evaluated computationally and is described only for completeness and as a possible program growth item.

If the cell and its neighbor are, for example, deep in the draw space, the appropriate interpolation index is $Q^* = \bar{Q}_1 - \bar{Q}_2$. If the guidances of the two cells are row-different or column-different, the switching crossover may be located in linear approximation by equating the linearly interpolated representation of Q^* for the two matrix elements in question, producing an interpolation scalar ζ , $0 \leq \zeta \leq 1$, which is the fraction of the distance between midpoints at which switching should occur. If the guidances are both row-different and column-different, the presence of two intersecting switching surfaces is implied. These are considered separately and the two ζ values averaged, in the approximation of present interest.

The computation of ζ values requires availability (storage) of the matrix elements and associated graduation indices. The storage requirement is substantial but temporary, hence the interpolation is done at the conclusion of each time-to-go "layer" during the buildup of active cells. Since each cell has as many as six neighbors, permanent core storage is provided for six ζ values, each rounded to three decimal digits.

If z_i , $i = 1, \dots, 3$, are cell-variable increments measured from the midpoint of the cell containing the current state-point, normalized to the distance between

the midpoint of the cell and the appropriate neighbor, then

$$p_i = \frac{|z_i|}{\zeta_i} \quad i = 1, \dots, 3$$

is useful for determining whether the guidance of the reference cell or that of one of its neighbors should be used. Three of the six ζ values stored are selected according to the signs of the components of z_i for use in computing the p_i . The p_i value is taken as zero where there is no neighbor or where the neighbor has the same guidance as the reference cell. If more than one of the three neighbors of interest has the same guidance, the p value for the two or three is determined jointly as

$$p = \sum_{j=1}^{k \leq 3} \frac{|z_i|}{\zeta_j}$$

which accounts for angling of the switch surface to the cell mesh. If all cell p_i calculated are $p_i \leq 1$, reference-cell guidance is used. If at least one $p_i > 1$, the guidance of the neighbor corresponding to the largest p_i is used.

Interpolation indices are employed as follows, according to the pairing of outcomes in the reference cell and the neighbor under examination:

1 & 1	time-to-capture
1 & 2	Q^*
1 & 3	\bar{Q}_2
1 & 5	\bar{Q}_1
2 & 2	time-to-capture
2 & 3	\bar{Q}_1
2 & 5	\bar{Q}_2
3 & 3	time-to-capture
3 & 5	Q^*
5 & 5	Q^*

The interpolation between active-cell midpoints is intended to produce the equivalent of a finer cell mesh, as far as steering errors are concerned, or, alternatively, permit the use of fewer cells for the same magnitude of error.

SECTION IX

DESCRIPTION OF EXAMPLES

In the first example to be described, Vehicle #1 has conventional weaponry, $\bar{r} = 2$ n. miles, and $\sigma = 10^\circ$. Vehicle #2 has identical weaponry, but in addition has wide-angle special weaponry, $\bar{r} = 1.5$ n. miles, and $\sigma = 60^\circ$. Vehicle #1, however, has slightly higher turn rates, both maximum instantaneous and sustainable, and more favorable energy rate at any given turn rate. Vehicle #1 is allowed a four-way choice: proportional navigation with any of three $\bar{\omega}$ values, maximum instantaneous, maximum sustainable, and zero; dash-away. Vehicle #2, who must win early or never, is restricted to choice between proportional navigation with maximum instantaneous and maximum sustainable rates, and dash-away. The engagement takes place with both craft at a specific energy of 31,000 ft. Speeds are around 1000 ft./sec., varying somewhat with choice of ω . The aircraft are those of Ref. 7. Of the twelve combinations of control options, five permit disengagement at various times before the 30 sec. cut-off that denotes a draw if no capture has taken place.

In the second example, the weaponry is the same as that just described; however, the performance and maneuverability characteristics are those of a different aircraft, a version of the F-5, and the opponents are identical.

SECTION X

SCORING

For a given set of initial conditions, the trajectories are calculated twelve times, once for each combination of control parameters, and the results arranged in matrix form, thus:

V_2	V_1			
	max toward	med toward	straight	turn-and-dash-away
max toward	3	3	2	5
med toward	3	3	2	2
turn-and-dash-away	1	1	4	5

Here "toward" implies proportional navigation.

Each matrix is scored twice, once with what might be called a minimax rule, again with a maximin rule. The first player chooses the column, the second the row, according to his preference order. In minimax, the first player is assumed to have chosen first; for each choice of column, the row choice is given by

[3 3 2 2]

The first player, anticipating this, would choose the outcome 3, the minimax score. In maximin, the second player is assumed to have chosen the row first. For each choice of row, the preference-ordered choice of column by the first player results in

$$\begin{bmatrix} 5 \\ 3 \\ 1 \end{bmatrix}$$

The second player's choice of row, in anticipation of this, is the outcome 5, the maximin score.

The terms minimax and maximin are employed very loosely here, as the game of interest is not naturally zero-sum unless player #1's preference order is the opposite of player #2's, and this does not arise naturally in familiar battle settings.

SECTION XI

GAME-SCORING ILLUSTRATIONS

Examples were sought which exhibit a variety of outcomes in the scoring matrix, yet do not have too many confusing guidance switchings brought about by the active-cell structure. It turns out that such cases are scarce and, finally, a six-second limit was imposed upon engagement duration in order to provide one. A second example, more interesting but slightly more complex, also features a six-second limit.

The first case chosen has the participants separated by just under 2 n. m. at the outset, each in the other's forward hemisphere. The maneuvers corresponding to the various elements in the matrix of initial guidance choices are sketched in the accompanying figure. The matrix is

$$\begin{bmatrix} 2 & 2 & 2 & 2 \\ 3 & 2 & 2 & 2 \\ 1 & 5 & 5 & 5 \end{bmatrix}$$

Here 1 = one-capture, 2 = two-capture, 3 = mutual capture, 4 = disengagement, and 5 = draw. No 4's occur on account of the short duration.

The maneuvers corresponding to each element of the matrix are noted on each of the dozen sketches of Fig. 3. There is nothing subtle about the interpretation: #2's best maneuver is a maximum-rate turn toward #1, which effects capture early no matter what maneuver #1 chooses (top row). Should #2 turn less vigorously (middle row), #1's best maneuver is a maximum-rate turn toward #2, and this results in a mutual capture. An evasive turn away from his opponent is a blunder for #2, as, in this event, #1 captures via his best maneuver, a maximum-rate turn toward #2 (bottom row).

Matrix scoring is carried out according to the preference orders 1, 4, 5, 3, 2 for #1 and 2, 5, 4, 3, 1 for #2. The general idea is similar to the "worst case" concept familiar from system design, although the closed-loop-control aspect, which makes the problem into a game, introduces subtle differences. None of these complicate the particular example, however.

#1 chooses the column of the matrix and #2 the row, each assuming the worst, from his own viewpoint, about the other's choice. A choice of a matrix element amounts to a particular selection from a four-way guidance choice by #1 and from a three-way choice by #2. Actually, it is only an initial selection; switchings in guidance take place as the point in joint state space moves through the active-cell structure. In the example, no switchings occur, except in the draw outcomes.

Looking at the matrix of outcomes, #1 reasons thus: if #2 turns away, I may choose between the outcomes of the bottom row and obtain a one-capture by opting to turn sharply toward #2; if #2 turns toward me at medium turn rate, my choice of outcomes in the middle row is again sharply toward, which effects a mutual capture; if #2 turns toward me at maximum rate, I am captured no matter what and choose my guidance for the longest time to capture in the top row (unfortunately, due to discretization, they are all two-second captures, and the choice of first column is made arbitrarily).

#2 can think through this before choosing the row; he is thus choosing between the elements of a column vector

$$\begin{bmatrix} 2 \\ 3 \\ 1 \end{bmatrix}$$

and the top element is his choice, this corresponding to a choice of top row in the matrix. The score of the matrix is 2, provided by the preference-ordered choice of first row, first column, which corresponds to both guidance choices of turn max toward. It happens that, in this particular engagement, the wide angle weaponry never comes into play. #2's win is due to a slight advantage in geometry at the beginning of the engagement.

A second example has the scoring matrix

$$\begin{bmatrix} 3 & 3 & 2 & 2 \\ 3 & 3 & 2 & 2 \\ 1 & 1 & 1 & 1 \end{bmatrix}$$

The trajectories are shown in Fig. 4. The outcome is mutual capture provided by second-row, second-column initial guidance choices. Although the confrontation is not head-on, it has the elements of a game of "chicken", made lethal by the reach of weaponry. If either vehicle turns away initially, and the other does not, the player turning away is captured. If both turn away initially, as in the lower right sketch, the geometrical situation shortly later favors #1, who captures irrespective of further evasion by #2. The active-cell guidance adopted subsequently by #2 merely prolongs the duration to capture. In the engagement under discussion, #2's wide-angle-weapon coverage is a decisive factor. Guidance switchings arising from passage of the trajectory pair through the cell structure are indicated on the trajectories by tick marks followed by the new guidance combination in use, the numbers 1 through 12 denoting the matrix-element combinations.

As in the preceding example, the first player chooses the column, the second the row, according to his preference order. In minimax, the first player is assumed to have chosen first; for each choice of column by #1, the choice by #2 is arrayed in a row as

$$[3 \quad 3 \quad 2 \quad 2]$$

The first player, anticipating this, would choose the outcome 3, the minimax score. In maximin, the second player is assumed to have chosen the row first. For each choice of row, the preference-ordered choice by the first player results in

$$\begin{bmatrix} 3 \\ 3 \\ 1 \end{bmatrix}$$

The second player, in anticipation of this, chooses the outcome 3, the maximin score. The terms minimax and maximin are employed loosely, as the game is not naturally zero-sum unless player #1's preference order is the opposite of player #2's, and this does not arise naturally in familiar battle settings. In the interest of more nearly unique determination of guidance options, graduated preferences are adopted within each category. Thus: minimax time in 1; maximin time in 2; maximum time in 3; reciprocity in 5 according to the scheme of the preceding section.

Close examination of individual encounters, such as the two just described, led to a modeling refinement, viz., a shift in preferences following a first capture so that the capturing player subsequently maximizes his own margin against capture. This change was found to reduce the number of mutual captures in a family of engagements by roughly 5 to 10%. The refinement is not incorporated in the results for a first example immediately following, but is incorporated in those for a second example to be presented in a later section.

SECTION XII

RESULTS FOR A FIRST EXAMPLE

Fourth-order Runge-Kutta integration with 1 sec. time steps were used. The interval of 3 sec. is used as a building-block for determining the active-cell structure. Results are calculated in each case for a specified initial separation and an assumed uniform distribution of both vehicle headings, every 15° around the clock. Combinations of headings producing initially positive range rate are screened out. In each case, a total of 335 engagements are calculated and scored.

The results for the first example to be presented illustrate the effects of gross modeling changes and were calculated without the active-cell structure, i. e., with no switchings between guidance laws, save for a switch to "breakaway" guidance by a capturing vehicle in an attempt to avert mutual capture. The following table presents results conveying an idea of the effectiveness of Vehicle #2's wide-angle weapon, the first column assuming the weapon inoperative, the second operative, both incorporating the maneuverability and performance penalties incidental to the weapon installation.

TABLE 1

EFFECT OF WIDE-ANGLE WEAPONRY

Outcome	2 n. mi. sep.	Wide-angle weapon inoperative	Wide-angle weapon operative
1 (1 captures)		130	73
2 (2 captures)		52	87
3 (mutual capture)		28	74
4 (1 disengages)		120	95
5 (draw)		5	6

As mentioned earlier, it is assumed that a mutual capture takes place if, within 3 sec. of a capture, a capture of the opposite type takes place, this accounting roughly for lag in weapon effectiveness (e.g., IR missile time-of-flight). The effect of reducing this 3 sec. mutual-capture period to zero is shown in the following table.

TABLE 2
EFFECT OF MUTUAL-CAPTURE PERIOD

Outcome \ 2 n. mi. sep.	3 sec. mutual-capture period	0 sec. mutual-capture period
1 (1 captures)	73	115
2 (2 captures)	87	121
3 (mutual capture)	74	13
4 (1 disengages)	95	80
5 (draw)	6	6

The effect is seen to be appreciable and warrants careful modeling.

It is noted that some of the captures in these and other results occur initially, before any evasive maneuver, and this is quite realistic; in fact, reality has a high incidence of such encounters, reflecting the advantage of surprise.

Table 3 shows the effect of eliminating the turn-and-dash-away guidance options for both vehicles. Elimination is seen to be of minor importance at an initial separation of 2 n. mi., but decisively in favor of the wide-angle-weapon-equipped vehicle at 4 n. mi. in sharply reducing the number of draws.

TABLE 3

EFFECT OF TURN-AND-DASH-AWAY OPTION

Separation Outcome	2 n. mi.		4 n. mi.	
	turn-and-dash-away optional	no turn-and-dash-away	turn-and-dash-away optional	no turn-and-dash-away
1 (1 captures)	73	76	0	0
2 (2 captures)	87	87	0	42
3 (mutual capture)	74	77	0	21
4 (1 disengages)	95	90	272.5	270
5 (draw)	6	5	62.5	2

Table 4 presents results with an active cell buildup based upon the mini-max rule in comparison with corresponding results obtained without the active cell structure. The reduction in the number of mutual captures is of particular interest. Results vary considerably with initial separation, as shown in Table 5,

TABLE 4

EFFECT OF ACTIVE-CELL STRUCTURE

Outcome	2 n. mi. sep.	with active cell structure	without active cell structure
1 (1 captures)		38	73
2 (2 captures)		109	87
3 (mutual capture)		16	74
4 (1 disengages)		127	95
5 (draw)		45	6

obtained employing the active-cell structure. The pattern of strategies emerging is of interest. For large initial separations, engagements tend to be head-on should both participants be aggressive, but this leads to mutual capture, which both rate very low in the assumed preference order. Hence, the outcomes tend to be mainly draws and disengagements. For very large separations, Vehicle #1 has ample time to gain energy prior to engagement, and therefore can insure a disengagement instead of a draw in a preponderance of cases. Large-separation scenarios are realistic only with assumed surface-radar assistance to furnish the equivalent of the required visibility; settings in which both vehicles are provided such assistance are relatively rare.

TABLE 5
EFFECT OF INITIAL SEPARATION DISTANCE

Outcome \ Separation	1 n. mi.	2 n. mi.	3 n. mi.	4 n. mi.
1 (1 captures)	113	38	32	2
2 (2 captures)	197	109	69	68
3 (mutual capture)	19	16	9	4
4 (1 disengages)	2	127	194	195
5 (draw)	4	45	31	66

Close-in, draws and disengagements occur less frequently, and mutual captures take place occasionally in spite of the assumed preference ordering. The wide-angle weaponry generally produces a high exchange ratio in favor of Vehicle #2. Dash-away is rarely adopted close-in as a means of retreat on account of vulnerability to the 2 n. mi. narrow-angle weaponry in a rectilinear tail chase.

The bulk of computational expense turns out to be in the building up of the active-cell structure; the expense of evaluation runs is relatively small, even for a large family of engagements. Expense rises sharply versus the maximum time of engagement specified; however, few additional capture cells are accumulated past 15 or 20 seconds. Probably the 30-sec. maximum time is excessive for applications of the kind typified by this example.

SECTION XIII

REPRISAL GUIDANCE

The subject of differential games is still young (Refs. 9, 10, 11), but much progress has already been made on its theory, and enough done with simple examples to tempt engineers and operations analysts into applications work. Applications thinking has been dominated, quite properly, by the problem of obtaining approximate solutions, either by simplification of system models or of solution procedures. Little attention has been paid so far to the exploitation of solutions already in hand for closed-loop control purposes. The present section looks at the possibility of removing some of the conservatism inherent in gaming calculations in pursuit/evasion applications. It owes much to discussions between the writers and Eugene Cliff of VPI.

It is basic to differential gaming that each participant plays optimally, any departure by one's opponent being assumed momentary and not worth considering for planning purposes. Control policies based upon the extrapolation of an opponent's current departures from optimality are sometimes called "reprisal strategies", and have not been widely studied. One extreme is extrapolation of an opponent's trajectory, under some plausible assumption about his controls, for purposes of solving one's own pursuit (or evasion) problem as an optimal-control problem. The other extreme attempts to exploit a real or perceived advantage in system-delay time (the sum of information-processing and control delays) based upon short-term considerations. For this, there is an applicable theory of upper and lower games (Ref. 11). Attention is directed in the following mainly to the practically important cases intermediate between these extremes.

There is an obvious additional margin to the informationally-advantaged player in a discretized sequential game, such as the present one, i. e., to the player who makes his choice with knowledge of his opponent's choice. In pursuit/evasion games, and in other differential games in which the Hamiltonian function

is separable, this advantage is supposed to disappear in the limit as the discretization time-increment shrinks to zero (Ref. 11). It appears, however, that the effect of nonzero time-step may be substantial. There is also an important related effect, viz., that the informationally-advantaged player must play closed-loop to retain his advantage. Otherwise, the use of open-loop-optimal strategy against nonoptimal play may result in penalties. The effect is equivalent to that of successful deception by his opponent.

A "reprisal" guidance policy, i.e., one which attempts to exploit perceived departures from optimality by one's opponent by extrapolation of his errors, may be synthesized via minor changes in the cell buildup process. If one assumes that errors will persist for a time period equal to the basic buildup time increment, for example, the procedure is to erase the top layer and rebuild it as many times as the opponent has guidance options, in each instance assuming that the opponent's freedom is restricted to the particular option. This generates several top layers, three or four in the example, to be used selectively depending upon the opponent's choice of control. If the opponent plays optimally, the guidance selected is optimal in the preference-ordered sense employed in the buildup. The risk lies entirely in the assumption that one's perception of the opponent's control is fast enough and accurate enough to trust.

Extrapolation of opponent's errors for a time spanning several layers of subcells is also possible and attractive; these layers are simply rebuilt the requisite number of times, assuming that the opponent's guidance is locked in to each choice in turn for the entire extrapolation time-span. In this case, the guidance generated is not optimal against optimal play; one cannot have everything. However, a compromise suggests itself, viz., use preference-ordered-optimal guidance when one's opponent is playing optimally — extrapolate only in the face of nonoptimal play. Such a mix might be called a minimax-reprisal composite.

SECTION XIV

ILLUSTRATIVE NUMERICAL RESULTS FOR REPRISAL GUIDANCE

The example is identical to that of Ref. 1 except that the speed and turn-rate characteristics of the two aircraft are equal — in the present case both are F-5's — and the disengagement outcome, a special type of draw, does not appear as a result of this. Aircraft #1 has a narrow-angle ($\pm 10^\circ$) weapon effective out to two nautical miles. Aircraft #2 has an identical weapon and, in addition, a wide-angle weapon (60° semi-apex angle) with a reach of 1.5 n. mi. There are 250 cells each partitioned into 10 subcells of 3-sec. time-remaining increment. A draw is declared if no capture has occurred by 27 seconds. The family of encounters for this example consists of the 250 cases initiated from the cell midpoints.

Table 6 summarizes results obtained for this family first under the assumption that both players make minimax control choices, the term being used here loosely to denote preference-ordered-optimal. These results indicate the sort of superiority for #2 that might be expected as a result of his weaponry advantage.

TABLE 6

EFFECT OF GUIDANCE OPTIONS

Outcome	Both minimax	#2 hard-turning #1 reprisal (3 sec.)	#2 hard-turning #1 reprisal (30 sec.)
1 (#1 captures)	21	18	19
2 (#2 captures)	91	84	68
3 (mutual capture)	30	39	35
5 (draw)	108	109	128

Results are also shown for two cases in which #2 is locked into hard-turning guidance toward his opponent. There is a shift in favor of #1, reflected in reduction in #2-captures, dramatic for the case of long-term extrapolation to T_{\max} as much as 30 seconds. The reduction in #1-captures is believed attributable to coarseness-of-mesh in combination with the fact that many draws are near-captures. It should be borne in mind that 85 of the captures occur initially, in the capture set: 10 #1-captures, 52 #2-captures, and 23 3-captures.

Trajectory comparisons are given in Fig. 5 for two cases in which #1 gains by long-term extrapolation (30-sec. reprisal). In Fig. 5A, minimax optimal play results in a 2 capture as a result of an initially gentle turn by #2 producing awkward geometry for #1, who turns away but cannot subsequently avoid #2's wide-angle weapon. In the case of hard-turning steering by #2, which is overly aggressive in the circumstances, #1, by turning to the attack, can effect a mutual capture. In Fig. 5B, minimax optimal play results in a scoreless tail chase, while hard-turning to the attack by #2 proves unwise, resulting in a 1 capture.

SECTION XV

ALTITUDE CHOICE AND "MAKING USE OF THE VERTICAL"

When the F-4 was first introduced into service, it flew in mock combat against the older F-8, not very successfully at first. Over a long period, literally years, the F-4 pilots gradually learned how to take advantage of the airplane's ability to reach higher energies than the F-8, and of its generally higher energy rate (specific excess power, P_g) by "making use of the vertical", until the F-8's turn-rate advantage in the "normal" altitude-airspeed range was eventually overcome (Ref.12). The evolution of good, or even improved, tactics evidently takes much longer than does training to execute currently-recommended tactics, especially where vertical-maneuvering aspects are important. It is suspected that the limited flight and simulator mock-combat experience with thrust-augmented-lift versus relatively high-powered conventional aircraft suffers from a fairly severe case of this same ailment.

The preference-ordered gaming work of Ref. 1 was inspired by results obtained on a two-cockpit simulator in the study of Ref. 7, which explored the potential of large-envelope wide-angle weaponry. No tendency to take the engagement to either extreme of altitude was noted in the simulation study, and this is perhaps attributable to a large extent to the briefing instruction: "be aggressive". The modeling of Ref. 1 is 2-D, except for deliberate disengagement to a high-energy haven, treated on a simplified basis. This resulted partly from the investigation's initial purpose, viz., to illuminate the simulation data, and was due partly also to a natural inclination to deal with the simpler problem first, deferring an attack on the 3-D problem.

In the following, the question of altitude choice will be taken up for the case of rôle-determined pursuit/evasion with "well-separated" geometry, i.e., each combatant initially well out of reach of the other's weaponry. The characteristics of the two aircraft of Ref. 1 will be used for example computations. As is usual

with gaming logic, the tactics emerging are sharply tailored to differences in the characteristics of the opposing vehicles and, in this sense, the findings are specialized. Yet the approach for a general pair of combatants will be apparent. The altitude-choice logic emerging is of interest for use in future application of gaming tactics to 3-D point-mass simulations.

Modeling attractive for gaming choice of altitude in the well-separated case is that of Ref. 13, based upon the Game of Two Cars. The scenario has the vehicles rôle-designated and initially arrayed line-astern. The evader allows the pursuer to approach to a certain distance, meanwhile adjusting his own altitude; then he executes a breakaway maneuver. If the evader's normal acceleration capability exceeds that of the pursuer, a miss develops whose horizontal component is estimated by Eq. (7) of Ref. 13:

$$\bar{R} = \frac{V_1^2}{2 V_2 \omega_2} - \frac{\pi}{2} \left(1 - \frac{\sqrt{2}}{2} \right) \frac{V_1}{\omega_1} \quad (14)$$

where V_1 and V_2 are true airspeeds of evader and pursuer, respectively, and ω_1 and ω_2 are their respective turn rates. The vertical component of the miss is the difference in altitudes, chosen by the pursuer. Two limiting cases for the vehicle speeds were examined in Ref. 13, the case of marginal overtaking speed and the case of a speed advantage chosen by the pursuer for maximum normal acceleration. A speed assumption appropriate to the present application is that both aircraft speeds are determined from current specific-energy values and choices of altitude. The pursuer's altitude-speed choice, constrained by a requirement that his speed equal or exceed the evader's, is made so as to minimize the root-sum-square of horizontal and vertical miss components.

If the joint state vector is within the "draw" region, an extended-duration chase is likely and, in this case, sustainable-acceleration figures are appropriate

for miss estimation. On the other hand, maximum-instantaneous-acceleration figures are applicable within a capture region in state space, or near its boundary.

Consider first the case of specific energies of the example aircraft equal at 31K, extended-duration assumptions, Aircraft #2 the pursuer and #1 the evader. In this setting, the relatively clean and light Aircraft #1 takes the chase to low altitude, drawing #2 down near his flight envelope's lower-limit altitude, approximately 4000 ft., generating a substantial sustainable-g deficiency and miss, about 2300 ft. (Fig. 6). If the pursuer has less specific energy than the evader, he finds himself worse off, as the requirement to at least match his speed to that of the evader forces him to descend below the evader to a region of high dynamic pressure and high drag. In the case of pursuer energy higher than the evader, computations by rote predict a serious problem by virtue of high drag; however, a little reflection shows that excess energy is easily disposable, in the particular scenario, by throttling and speed-braking, and that, furthermore, some can be traded advantageously for higher-than-sustainable turn rate. So the worst case for the evader is pursuer energy slightly higher than his own.

In the case of not-quite-so-well-separated geometry, capture possibly imminent, similar miss computations carried out with maximum instantaneous turn rates are of interest. The pursuing Aircraft #2's weight disadvantage enters the miss computations, but his drag disadvantage does not. However, when the miss is small or zero, the drag disadvantage, of course, influences the energy-rate comparison that decides the evasion altitude. With equal energies, the miss is small over the entire altitude range; the maximum is 300 ft. at the upper limit of the flight envelope, approximately 27,000 ft., where there is a 500 ft./sec. energy-rate margin in favor of the evader. With a pursuer

energy disadvantage, the greatest miss occurs for the same high-altitude choice, and the miss slightly exceeds the energy difference. If the pursuer has an energy advantage, descent to the lower reaches of the envelope becomes attractive, primarily on energy rate.

With the relatively heavy and aerodynamically dirty Aircraft #2 as evader, dominating the choice of altitude, well-separated engagements find the evader moving aloft to the top of this flight envelope. With energies equal to 31K, or with a pursuer energy advantage, the miss estimate, employing sustainable turn rates, is zero over the whole altitude range and the evader's choice of the upper end is made by comparing energy rates. If the pursuer has an energy deficiency, the miss is constant at the value of the energy difference over the altitude range, and again the energy-rate balance decides. The balance is unfavorable to the evader over the whole altitude range, but it is least unfavorable at the high end. Similar results emerge when maximum-instantaneous-rate turns are assumed. The long-term trend in the draw space is against the evader.

SECTION XVI

POINT-MASS SIMULATION

The equations of motion, data representation, and control logic for the one-on-one point-mass-modeled air-combat simulation are described in the following.

1. EQUATIONS OF MOTION

Motion of each aircraft satisfies a constant-mass three-degree-of-freedom system of differential equations as follows:

$$\dot{h} = V \sin \gamma$$

$$\dot{\gamma} = \frac{g \cos \mu}{WV} (L + T_{\eta} \sin \alpha) - \frac{g}{V} \cos \gamma$$

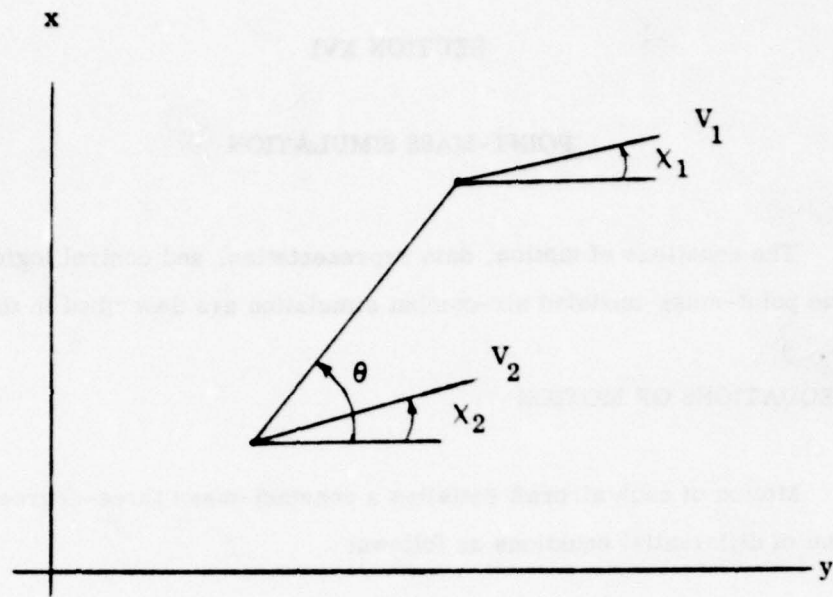
$$\dot{E} = \frac{V T_{\eta} \cos \alpha}{W} - \frac{V D}{W}$$

$$\dot{\chi} = \frac{g (L + T_{\eta} \sin \alpha) \sin \mu}{V W \cos \gamma}$$

$$\dot{x} = V \cos \gamma \sin \chi$$

$$\dot{y} = V \cos \gamma \cos \chi$$

Here h is altitude, γ flight-path angle to the horizontal, $E = h + \frac{V^2}{2g}$ specific energy, V velocity magnitude, χ heading angle, x and y horizontal position components, μ bank angle, T maximum thrust, η , $0 \leq \eta \leq 1$, throttle setting, L lift, D drag, and α angle of attack. Geometry in the horizontal plane, as viewed from above, is shown in the following sketch.



The bearing angle θ is defined by eq. (11).

2. DATA REPRESENTATION

Maximum engine thrust $T(M, h)$ is represented as a function of Mach number M and altitude h via double-table-lookup featuring a rectangular array and cubic-spline-lattice interpolation (Ref. 14). Lift and drag are given by

$$L = qSC_L = qSC_L \alpha$$

$$D = qS[C_{D_o} + C_{D_{C_L^2}} C_L^2 + \sigma C_{D_R}]$$

The lift is modeled as linear with angle of attack, α , and the drag quadratic with lift coefficient C_L . C_{D_B} is drag increment due to fully extended speed brakes; the brake setting is σ , $0 \leq \sigma \leq 1$. Zero-lift drag coefficient $C_{D_0}(M)$ is represented as a tabular function of M , with cubic-spline interpolation. The drag increment C_{D_B} is taken as a fixed fraction (input) of C_{D_0} . The drag-due-to-lift coefficient $C_{D_{C_L^2}}(M)$ is a tabular function of M with spline interpolation.

3. BANK-ANGLE LOGIC

For a hard-turning mode, the lift coefficient C_L is taken as

$$C_{L_M} = \min \left(\hat{C}_L, \frac{\bar{n} W}{qS} \right)$$

Here $\hat{C}_L(M)$ is maximum lift coefficient, a splined tabular function of M , and \bar{n} is structural limit load factor.

For a sustainable-turn mode, C_L is taken as

$$C_{L_{ss}} = \min \left(\hat{C}_L, \frac{\bar{n} W}{qS}, C_{L_s} \right)$$

where C_{L_s} is the lift coefficient for sustainable turning, approximated as that for $T=D$,

$$C_{L_s} = \sqrt{\frac{T}{qS C_{D_{C_L^2}}} - \frac{C_{D_0}}{C_{D_{C_L^2}}}}$$

With $\Delta x \equiv x_2 - x_1$, $\Delta y = y_2 - y_1$, and $\Delta h = h_2 - h_1$, the pursuit plane for Vehicle 1 is defined as the plane containing the line of sight and the opponent's velocity vector. The slope of the plane containing the line of sight and Vehicle 2's velocity vector is

$$s_2 = \sqrt{\frac{(\Delta h \dot{y}_2 - \Delta y \dot{h}_2)^2 + (\Delta x \dot{h}_2 - \Delta h \dot{x}_2)^2}{(\Delta x \dot{y}_2 - \Delta y \dot{x}_2)^2}}$$

The component of gravity normal to this plane is $g / \sqrt{1 + s_2^2}$ and the bank angle μ_{1p}^* required to balance this component of gravity is

$$\cos \mu_{1p}^* = \frac{W_1}{(L_1 + T_1 \sin \alpha_1) \sqrt{1 + s_2^2} \cos \gamma_1} \leq 1$$

If $\frac{W_1}{(L_1 + T_1 \sin \alpha_1) \sqrt{1 + s_2^2} \cos \gamma_1} > 1$, $\cos \mu_{1p}^* = 1$. Here L_1 and α_1

are the lift and angle of attack of the first vehicle. The sense of the bank angle μ_{1p}^* is determined by

$$\mu_{1p}^* \leq 0 \quad \text{if} \quad \pi \geq \chi_1 - \theta + \pi \geq 0$$

$$\mu_{1p}^* \geq 0 \quad \text{if} \quad 0 \geq \chi_1 - \theta + \pi \geq -\pi$$

where the test quantity has been defined to lie in the range $\pi \geq \chi_1 - \theta + \pi \geq -\pi$ by the addition of an appropriate integer multiple of 2π .

The corresponding definitions of s_1 and μ_{2p}^* are given by

$$s_1 = \sqrt{\frac{(\Delta h \dot{y}_1 - \Delta y \dot{h}_1)^2 + (\Delta x \dot{h}_1 - \Delta h \dot{x}_1)^2}{(\Delta x \dot{y}_1 - \Delta y \dot{x}_1)}}$$

$$\cos \mu_{2p}^* = \frac{W_2}{(L_2 + T_2 \sin \alpha_2) \sqrt{1 + s_1^2} \cos \gamma_2} \leq 1$$

$$\text{If } \frac{W_2}{(L_2 + T_2 \sin \alpha_2) \sqrt{1 + s_1^2} \cos \gamma_2} > 1, \cos \mu_{2p}^* = 1.$$

$$\mu_{2p}^* \geq 0 \quad \text{if} \quad 0 \geq \chi_2 - \theta \geq -\pi$$

$$\mu_{2p}^* \leq 0 \quad \text{if} \quad \pi \geq \chi_2 - \theta \geq 0$$

It is of future interest to construct a one-on-one point-mass-modeled simulation program employing control logic along the general lines of Ref. 1 and the present section, i. e., control policies patched together selectively from precalculated gaming computations carried out with various simplified models. 2-D Game-of-Two-Cars modeling, as in Ref. 1, will apply for nearly-equal energies and well-determined rôles, i. e., within the capture regions of active-cell structure which has been precalculated at two or more equal-energy points assuming "corridor" altitudes. The reference plane of the 2-D maneuvering will not, in general, be horizontal but will derive from 3-D orientation of velocity vectors. When one combatant has an energy advantage, the evader's altitude command will be biased in the direction of the altitude-choice logic of the preceding section, for well-separated geometry, and similar logic worked out for close-in geometries using "scissors" and "turning-game" (Ref. 3) modeling.

SECTION XVII

CELL BUILDUP AND EVALUATION PROGRAM

Four turn rates are input for Vehicle #1: maximum instantaneous, maximum sustainable, zero ("straight-flight" option), and maximum instantaneous again ("turn-and-dash-away" option). These are calculated separately, with velocity values corresponding to constant specific-energy, altitude unrestricted. There are three turn rates for Vehicle #2; the "straight-flight" option is missing. If the best-turn and best-dash altitudes for the two opposing aircraft do not come out reasonably close (as they have in the examples reported), a compromise is required to force the scenario into 2-D.

The program flows in the following manner. Input is read in via NAMELIST INP and then written out. If IPC equals zero, there are no existing cells and the program proceeds to generate a set of cells according to input specifications with NRT, NXT1, and NXT2 determining the number of cells to be generated. Using the initial conditions of the centers of all the cells, the capture set is found. If the center of a cell results in a mutual capture, the cell is assigned a 3 for capture and 0 for guidance, then is added to the capture set. If the center of a cell indicates a 1 or a 2 capture, then 12 three-second trajectories are integrated and, depending upon input, either a minmax or maxmin solution of the resultant matrix determines the row and column to be used for guidance, filling all ten layers of the cells with these values. This completes the capture set. The rest of the cells are generated, layer by layer, using different sets of trajectories. Beginning with starting time, TZERO, equal to the shortest time-to-go value at the outset, it is then successively decreased by three-second increments until TZERO = 0.

It is not necessary to build all the layers in one run. The cells are saved, after each layer has been completed, in a temporary file called TAPE1 internally.

The cell buildup terminates after an input number of layers have been accumulated (maximum = 10). During this time, primary as well as secondary, or reprisal, cells are built (according to an input trigger). If the cells are being built piecemeal, one has to make sure that the various options used are exactly alike, to avoid getting a mixed bag. (See INPUT section: IFN, LGI, MTPL, MMID, specifically.) NAMELIST INP2 is used when the cell buildup is a continuation of a previous partial buildup or if evaluation trajectories are required. Some items are repeated in both namelists in order to facilitate printing of input data.

Three different evaluation runs are made.

1. Evaluates all combinations of initial x_1 's and x_2 's from input tables of x_1 and x_2 .
2. Evaluates trajectories starting in the center of selective cells.
3. Evaluates trajectories starting in the center of each cell.

Each run prints a matrix of predicted outcomes vs. actual results in addition to a summary total for each capture type. A diagonal matrix indicates that all the predictions were satisfied.

The input required for use of the program is defined in the following section.

SECTION XVIII

INPUT

Definitions of the various input quantities required for operation of the cell buildup and evaluation program are listed below.

NAMELIST INP

		<u>Default</u>
X1	= x component of Vehicle #1	0.
Y1	= y component of Vehicle #1	0.
X2	= x component of Vehicle #2	0.
Y2	= y component of Vehicle #2	0.
C	= navigation ratio; used in $\dot{\chi} = C\dot{\theta}$	0.
NPRN	= incremental number of integration steps - used to obtain a detailed printout every NPRN integration steps	10000.
DELI	= initial integration interval	0.
R1B	= radius of capture for Vehicle #1	12152.231
R21B	= radius of capture of Weapon 1 for Vehicle #2	12152.231
R22B	= radius of capture of Weapon 2 for Vehicle #2	9114.173248
SIG1	= angle of capture for Vehicle #1	10. ⁰
SIG21	= angle of capture of Weapon 1 for Vehicle #2	10. ⁰
SIG22	= angle of capture of Weapon 2 for Vehicle #2	60. ⁰
NEQ	= number of equations to be integrated	6
V1T(12)	= velocities for Vehicle #1 - one for each element in the matrix	0.
XBD1T(12)	= $\frac{1}{\chi}$'s for Vehicle #1	0.

		<u>Default</u>
V2T(12)	= velocities for Vehicle #2	0.
XBD2T(12)	= $\dot{\chi}$'s for Vehicle #2	0.
TMXT(12)	= maximum time for each element in the matrix used for evaluating 4's	0.
NXI1	= number of entries in XI1T table	0
NXI2	= number of entries in XI2T table	0
XI1T(40)	= table of initial χ_1 for evaluation runs	
XI2T(40)	= table of initial χ_2 for evaluation runs	
TMXM	= global TMAX - maximum time for each trajectory	
C2	= used in eq. (8)	0.
NRT	= number of entries in RTBL	0
NXT1	= number of entries in XI1TB	0
NXT2	= number of entries in XI2TB	0
RTBL(5)	= radii representing endpoints in cell structure	0.
XI1TB(14)	= values of $\pi - \chi_1 + \theta$ for endpoints in cell structure	0.
XI2TB(10)	= values of $\chi_2 - \theta$ for endpoints in cell structure	0.
ITCI	= number of top layer to be generated during cell buildup	2
IPR	$\neq 0$ prints cells =0 suppresses cell print	1
IPC	=0 start cell buildup =251 for continued buildup and evaluations	0
IPL1(5)	= preference order when scanning rows	1, 4, 5, 3, 2
IPL2(5)	= preference order when scanning columns	2, 5, 4, 3, 1
C3	= used in eq. (9)	1000.

		<u>Default</u>
LCOP	= 1 or 2 - minmax is used for score	0
	= 3 or 4 - maxmin is used for score	
RTM(5)	= radii representing midpoints of cells	0.
X1TM(14)	= values of $\pi - \chi_1 + \theta$ for midpoints of cells	0.
X2TM(10)	= values of $\chi_2 - \theta$ for midpoints of cells	0.
IFN	= 0 - use reprisal set of cells	1
	= 1 - use primary and secondary cells	
	= 2 - use primary cells only	
CON12	= constant for choosing Q^* logic during minmax or maxmin evaluations	1, 2
LGI	= 0 - normal guidance	0
	= 1 - override with first column guidance	
	= 2 - override with first row guidance	
MTPL	= 0 - normal buildup	0
	= 3 - first column only	
	= 4 - first row only	
MMID	= 0 - no reprisal cells	0
	= 3 - reprisal buildup with first column guidance	
	= 4 - reprisal buildup with first row guidance	
K3	= number of seconds for blinding contestants	3

NAMELIST INP2

		<u>Default</u>
ITCP	= number of last layer generated for pickup of cell buildup	0
LCNP	= number of cells in capture set	0
LCN	= total number of cells generated + 1	2
MGLTR	= 0 - normal run	0
	= 7 - evaluation starting from center of cells	
K3	= number of seconds for blinding contestants	3
LGI	= 0 - normal guidance	0
	= 1 - override with first column guidance	
	= 2 - override with first row guidance	
IFN	= 0 - use reprisal set of cells	1
	= 1 - use primary and secondary cells	
	= 2 - use primary cells only	
TZRN	= starting and zero times for evaluation runs	0.
MMID	= 0 - no reprisal cells	0
	= 3 - reprisal buildup with first column guidance	
	= 4 - reprisal buildup with first row guidance	
MTPL	= 0 - normal buildup	0
	= 3 - first column only	
	= 4 - first row only	

SECTION XIX

CONCLUDING REMARKS

The use of the preference-ordered gaming model in the present application was inspired by manned simulation (Ref. 7) results obtained on a two-cockpit simulator exploring the potential of large-envelope wide-angle weaponry. The sparse, but impressive, results suggested that rôle-determination decisions are crucial and that engagements, when decisive, are over very quickly with such weaponry. The preference-ordered gaming results correlated qualitatively with those of the manned simulations. The gaming model seems well suited to the study of next-generation air-to-air weaponry, which tends to be large-envelope, wide-angle, high P_K , all-aspect.

The results of the present study suggest that departures from optimality in the details of air-combat maneuvers are not as important as are mistakes in deciding whether to attack, to flee, or to maneuver for an improvement in the situation relative to one's opponent without committing one's self to an attack. A rationale for rôle-determination, and for maneuvering in draw situations is furnished by the "threat-reciprocity" concept. The preference-ordered discrete-gaming computational approach in combination with "reprisal" technique for exploiting the mistakes of one's opponent by extrapolation seems promising for applications work.

The short-term emphasis in future work should be upon streamlining the computations and upon systematic exploration of mesh-size effects, mesh-interpolation, and the effect of informational advantage. A development of particular interest is the blending of the 2-D cell-structure control logic with altitude logic, along the lines discussed herein, into a 3-D point-mass digital simulation. This would provide a simulation model faithful to design details with decision and control logic having a basis in game theory, a combination hitherto unrealized. In conjunction with manned simulation,

the model would likely prove useful for study of air tactics, and possibly for training. Additional control logic could be provided in the cell structure, to permit extrapolation of opponent's errors, particularly rôle-decision blunders, for various assumed periods in study and training exercises.

An exciting possibility is application to 2-on-1 and, ultimately, to many-on-many. The advances presently reported fall precisely in the weakest area of existing air-combat simulation technology, viz., control logic. Serious enough for 1-on-1, this weakness becomes overwhelming for the many-on-many case. The attractive approach is the use of 1-on-1 results for instantaneous evaluation of the threat posed by each vehicle in the fray to each opponent, and the rational assignment of rôles and individual opponents, with particular regard to weaknesses of, and tactical blunders by, the opposition.

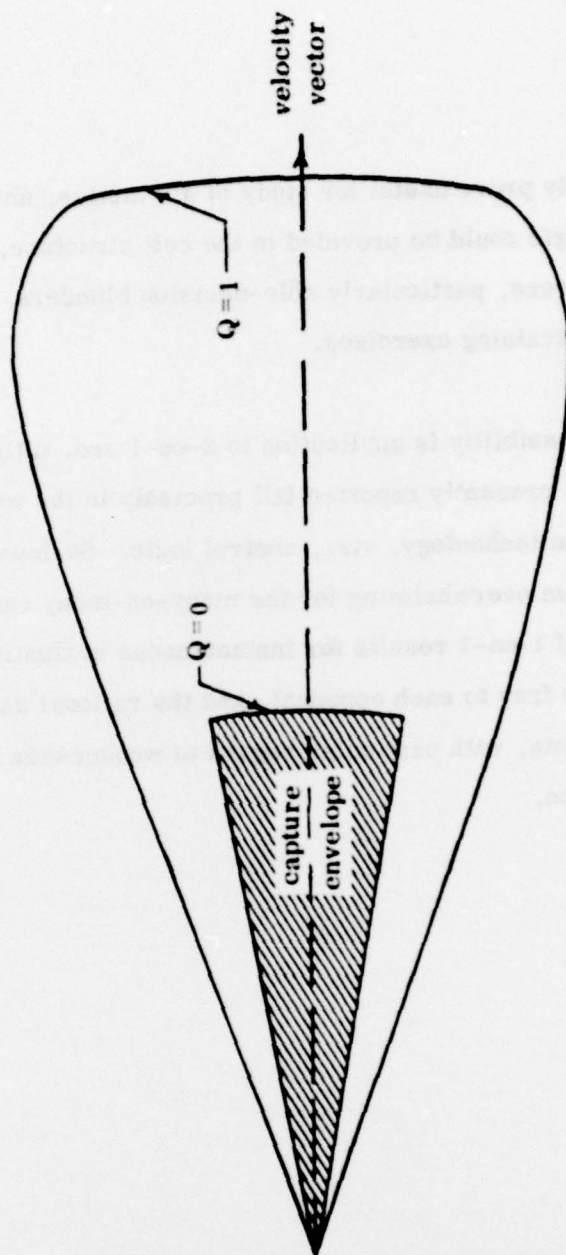


Figure 1. Generalized Miss

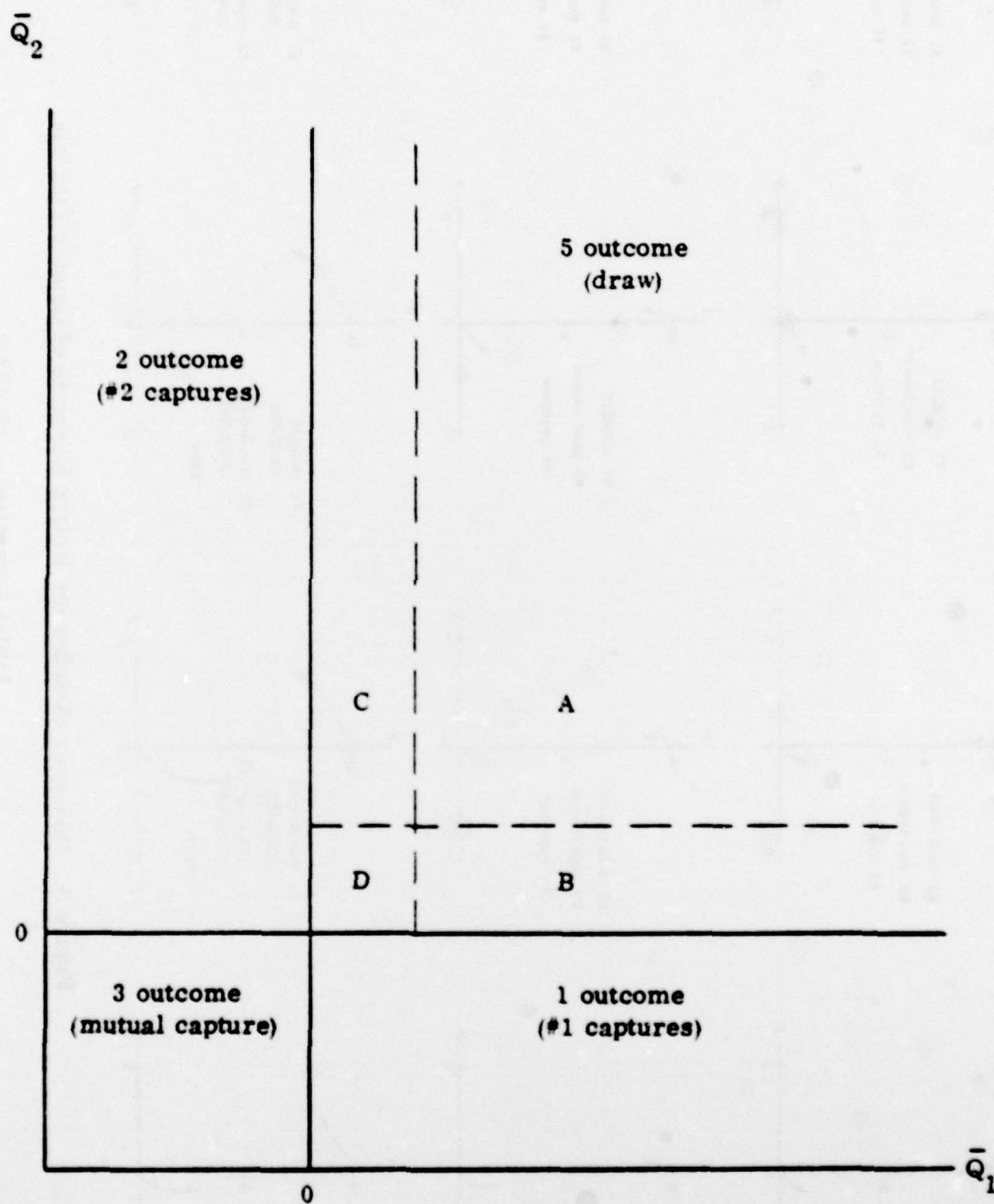


Figure 2. Capture and Draw Regions in \bar{Q}_1, \bar{Q}_2 Space

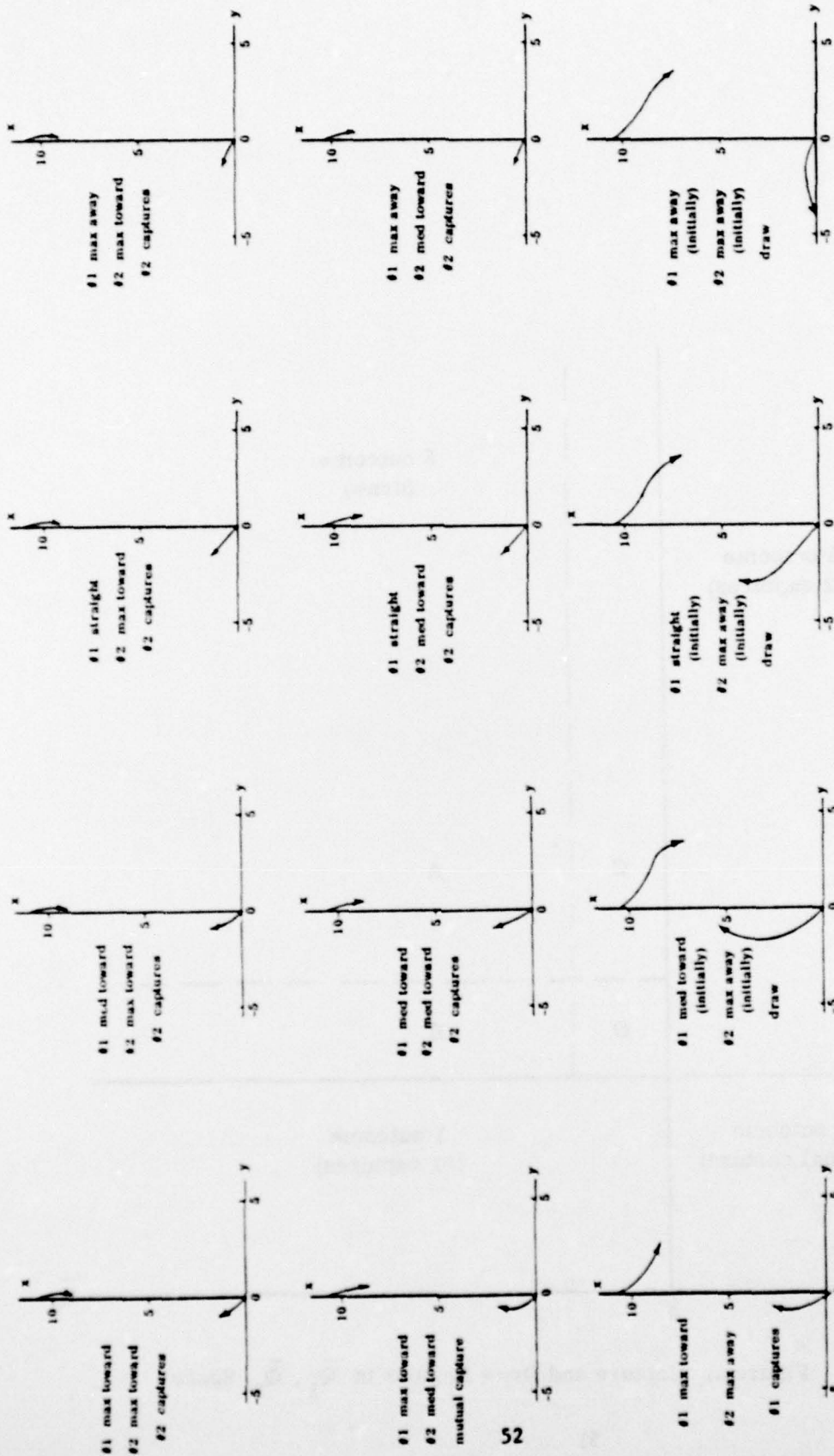


Figure 3. Maneuver Sketches for Matrix Elements of Gaming Example

Initial Separation 10,633 ft.
 #1 Heading 2.4 rad.
 #2 Heading -1.18 rad.

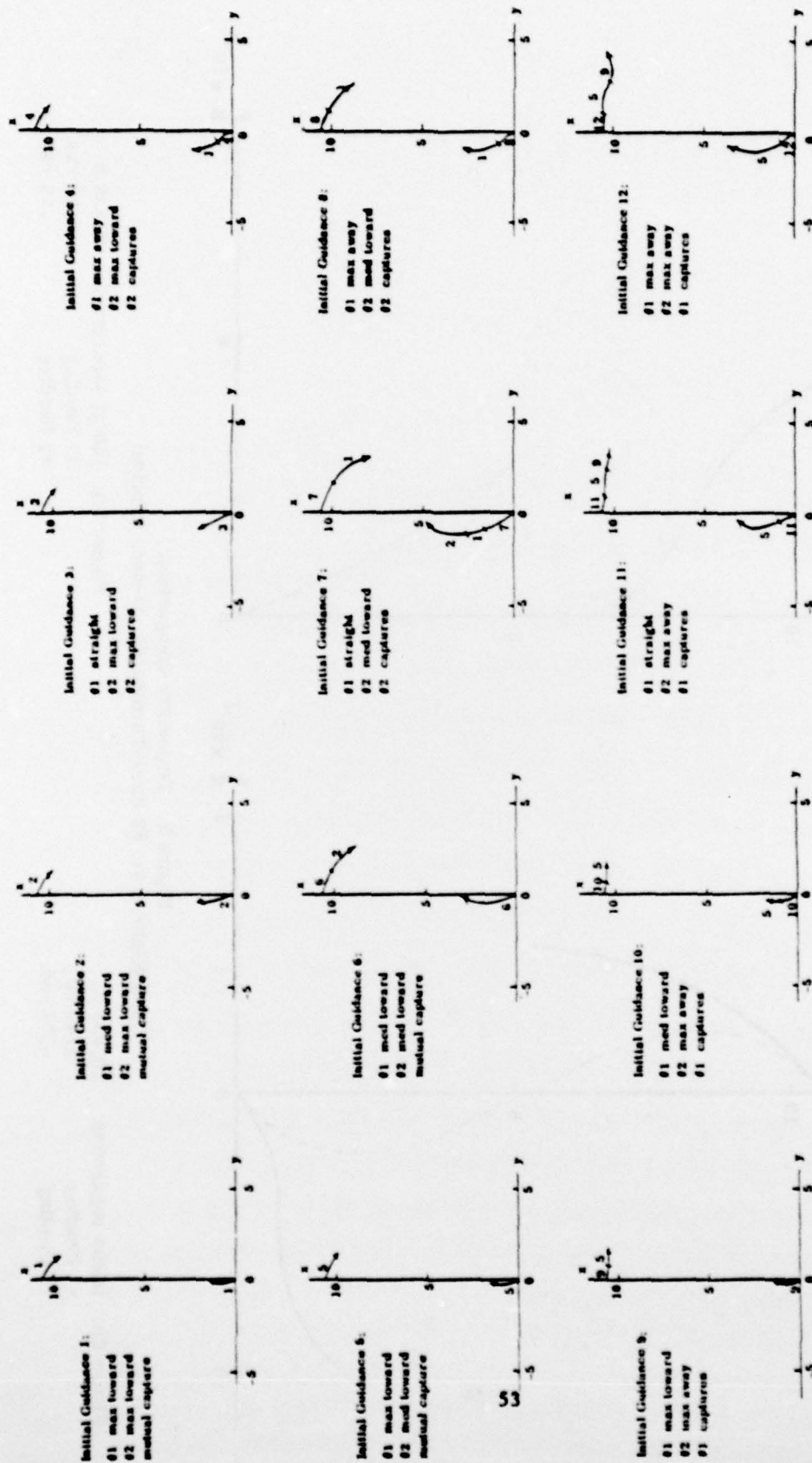
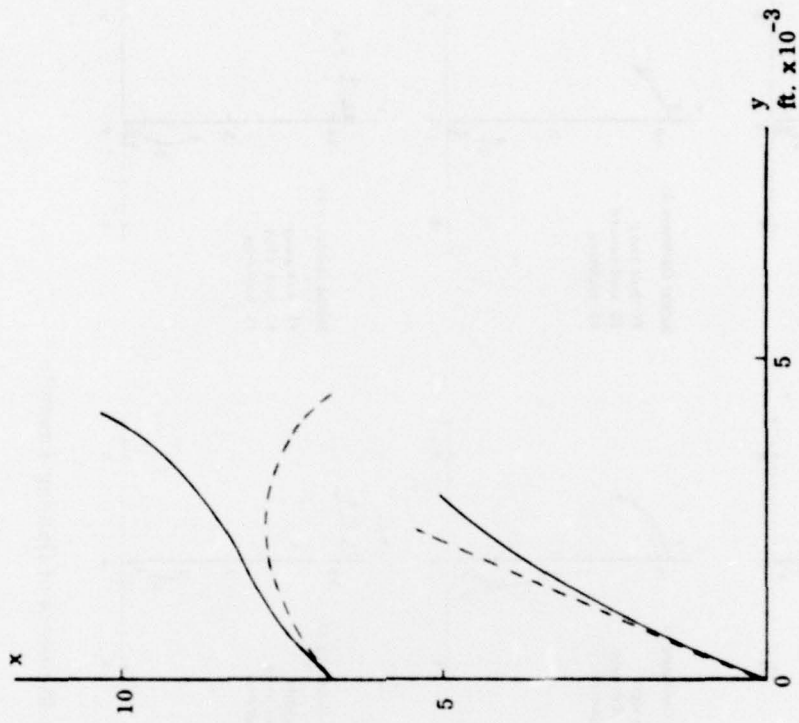


Figure 4. Maneuver Sketches for Matrix Elements of Gaming Example

Initial Separation 10,633 ft.
#1 Heading 1.96 rad.
#2 Heading -.26 rad.

--- #2 hard-turning/#1 30-sec. reprisal (1-outcome)
 --- both minimax (5-outcome)



--- #2 hard-turning/#1 30-sec. reprisal (3-outcome)
 --- both minimax (2-outcome)

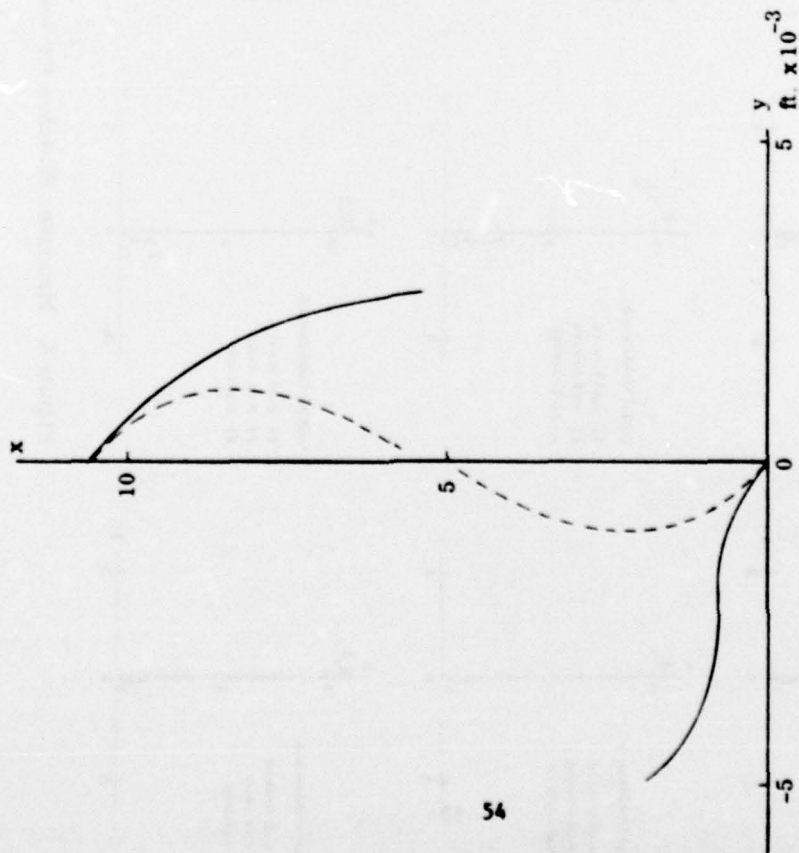


Figure 5. Trajectory Comparison
Both Minimax vs. #2 Hard-Turning/#1 30-sec. Reprisal

Figure 5A. Initial separation 10,633 ft.
 #1 Heading 2.40 rad.
 #2 Heading -.74 rad.

Figure 5B. Initial separation 6,836 ft.
 #1 Heading 1.18 rad.
 #2 Heading .79 rad.

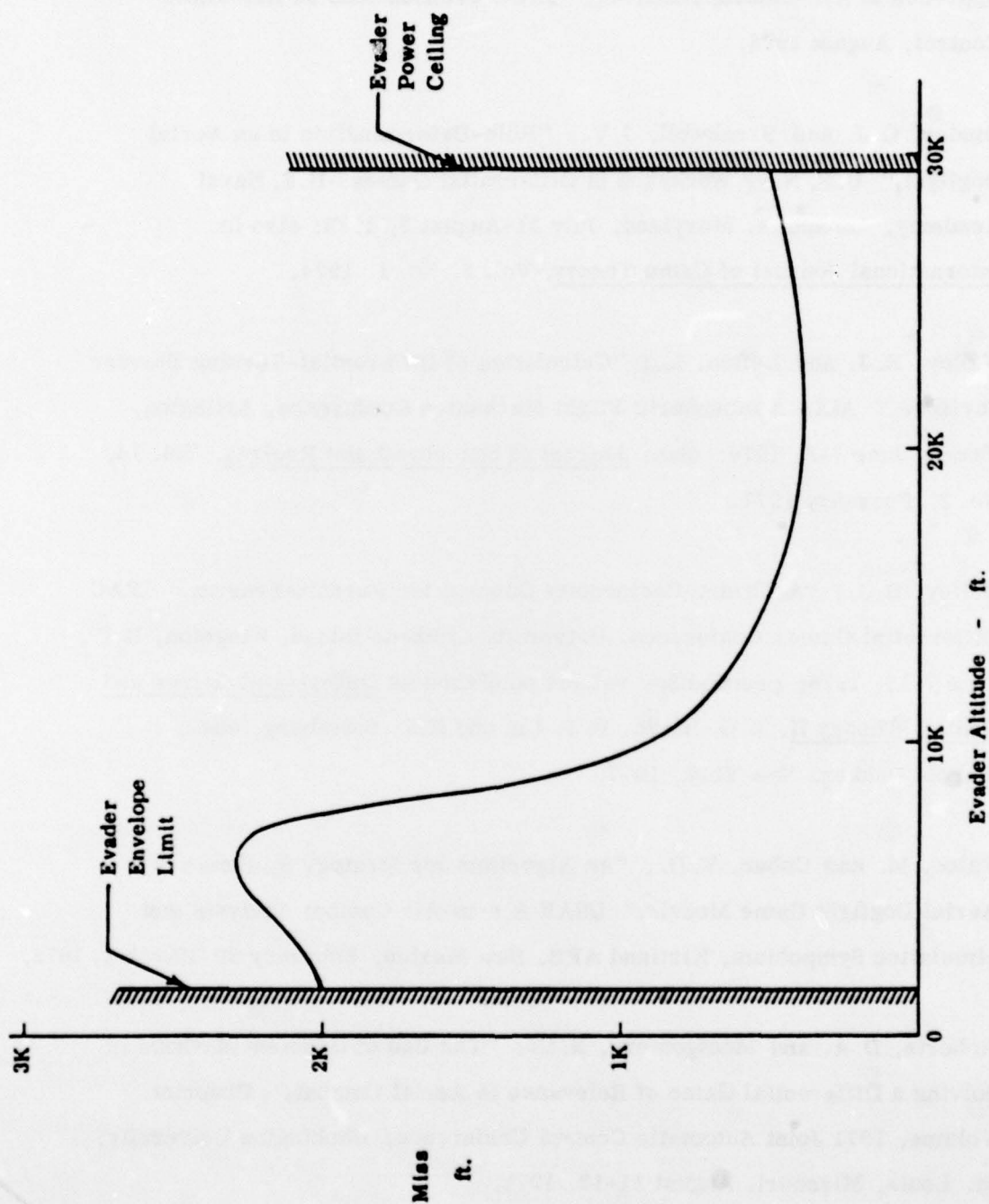


Figure 6. Breakaway Miss vs. Altitude Sustainable Turns
Pursuer/Evader #2/#1

REFERENCES

1. Kelley, H.J. and Lefton, L.; "A Preference-Ordered Discrete-Gaming Approach to Air-Combat Analysis," IEEE Transactions on Automatic Control, August 1978.
2. Olsder, G.J. and Breakwell, J.V.; "Rôle-Determination in an Aerial Dogfight," U.S. Navy Workshop in Differential Games, U.S. Naval Academy, Annapolis, Maryland, July 31-August 3, 1973; also in International Journal of Game Theory, Vol. 3, No. 1, 1974.
3. Kelley, H.J. and Lefton, L.; "Calculation of Differential-Turning Barrier Surfaces," AIAA Atmospheric Flight Mechanics Conference, Arlington, Texas, June 7-8, 1976; also, Journal of Spacecraft and Rockets, Vol. 14, No. 2, February 1977.
4. Kelley, H.J.; "A Threat-Reciprocity Concept for Pursuit/Evasion," IFAC Differential Games Conference, University of Rhode Island, Kingston, R.I., June 7-10, 1976; proceedings volume published as Differential Games and Control Theory II, E.O. Roxin, P.T. Liu and R.L. Sternberg, eds., Marcel Dekker, New York, 1977.
5. Falco, M. and Cohen, V.D.; "An Algorithm for Strategy Synthesis in Aerial Dogfight Game Models," USAF Air-to-Air Combat Analysis and Simulation Symposium, Kirtland AFB, New Mexico, February 29-March 2, 1972.
6. Roberts, D.A. and Montgomery, R.C.; "The Use of Gradient Methods in Solving a Differential Game of Relevance in Aerial Combat," Preprint Volume, 1971 Joint Automatic Control Conference, Washington University, St. Louis, Missouri, August 11-13, 1971.

REFERENCES (cont'd)

7. Newberry, C. H. ; Discussions at USAF Weapons Laboratory, Kirtland AFB, New Mexico, mid-1976.
8. Kopp, R. E. ; "The Numerical Solution of Discrete Dynamic Combat Type Games," in Techniques of Optimization, A.V. Balakrishnan, ed. , Academic Press, New York, 1972.
9. Isaacs, R. ; Differential Games, Wiley, New York, 1965.
10. Isaacs, R. ; "The Past and Some Bits of the Future," in The Theory and Application of Differential Games, J.D. Grote, ed. , Reidel, Dordrecht, 1975.
11. Friedman, A. ; Differential Games, Wiley-Interscience, New York, 1971.
12. Private communication with Gary Hill (NASA-Ames engineer and A-7 pilot), April 1976.
13. Kelley, H.J. and Lefton, L. ; "Estimation of Weapon-Radius Versus Maneuverability Tradeoff for Air-to-Air Combat," ALAA Journal, Vol. 15, No. 2, February 1977.
14. Mummolo, F. and Lefton, L. ; "Cubic Splines and Cubic-Spline Lattices for Digital Computation," Analytical Mechanics Associates, Inc. , Report Number 72-28, July 1972, revised December 1974.